Carbide-Derived Carbons with Tunable Porosity
Optimized for Hydrogen Storage

DE-FC36-04GO14282
October 2004 – September 2009

PI: Prof. John E. Fischer
Department of Materials Science and Engineering
University of Pennsylvania
3231 Walnut St.
Philadelphia PA 19104-6272
Phone: (215) 898-6924
Fax: (215) 573-2128
Email: fischer@seas.upenn.edu
http://www.seas.upenn.edu/~jefnano/

Co-PI: Prof. Yury Gogotsi
Department of Materials Science and Engineering
Drexel University
3141 Chestnut Street
Philadelphia PA 19104
Phone: (215) 895-6446
Fax: (215) 895-6760
Email: gogotsi@drexel.edu
http://nano.materials.drexel.edu

Co-PI: Dr. Taner Yildirim
National Institute of Standards and Technology
100 Bureau Dr, MS 8562
Gaithersburg, MD 20899-8562
Phone: (301) 975-6228
Fax: (301) 921-9847
Email: taner@nist.gov
http://www.ncnr.nist.gov/staff/taner

Collaborating Team Members:
Prof. Paolo Columbo, University of Padova (Italy)
Prof. Keith Gubbins, N.C. State University
Dr. Jacek Jagiello, ex-Quantachrome Inc.
Prof. Angel Linares-Solano, Alicante University (Spain)
Dr. Anna Llobet, Los Alamos National Laboratory
Dr. Jason Simmons, NIST

EXECUTIVE SUMMARY

On-board hydrogen storage is a key requirement for fuel cell-powered cars and trucks. Porous carbon-based materials can in principle adsorb more hydrogen per unit weight at room temperature than liquid hydrogen at -176 ^{o}C. Achieving this goal requires interconnected pores with very high internal surface area, and binding energies between hydrogen and carbon significantly enhanced relative to H_2 on graphite. In this project a systematic study of carbide-derived carbons, a novel form of porous carbon, was carried out to discover a high-performance hydrogen sorption material to meet the goal. We were unable to improve on the state of the art in terms of stored hydrogen per unit weight, having encountered the same fundamental limit of all porous carbons: the very weak interaction between H_2 and the carbon surface. On the other hand we did discover several strategies to improve storage capacity on a *volume* basis, which should be applicable to other forms of porous carbon.

Further discoveries with potentially broader impacts include

- Proof that storage performance is not directly related to pore surface area, as had been previously claimed. Small pores (< 1.5 nm) are much more effective in storing hydrogen than larger ones, such that many materials with large total surface areas are sub-par performers.

- Established that the distribution of pore sizes can be controlled during CDC synthesis, which opens the possibility of developing high performance materials within a common family while targeting widely disparate applications. Examples being actively pursued with other funding sources include methane storage, electrode materials for batteries and supercapacitors with record high specific capacitance, and perm-selective membranes which bind cytokines for control of infections and possibly hemodialysis filters.

RESULTS AND DISCUSSION

Preamble: Controlled porosity in CDCs

The motivation for this project was provided by a proof-of-concept experiment which established the principle of pore size tuneability by varying the synthesis conditions of a carbide-derived carbon [1]. The ternary carbide Ti_3SiC_2 in powder form was converted to amorphous carbon by heating in chlorine flow at temperatures from 300 to 1100 ^{o}C. Differential pore size distributions (PSD) were derived from gas sorption isotherms using N_2, Ar and CH_3Cl to accurately cover a wide range of pore sizes D. The results are shown in Figure 1. Up to 700 ^{o}C the PSDs indicate a monodisperse group of sub-nm pores with average diameters increasing systematically with increasing chlorination temperature

T(Cl). At higher temperatures, Fig. 1b), we observe a second group of larger pores which grow at the expense of the micropores, eventually dominating the PSD. Weight loss and energy-dispersive X-ray spectroscopy (EDS) analysis of the samples after chlorination suggested almost complete removal of Ti and Si above 400 °C. Because the CDCs retained the original volume of the carbide precursor, it is fair to assume the total pore volume to be the same after chlorination at different temperatures. The maximum pore volume of ~0.64 cm^3/g accessible to Ar and N_2 in CDC after heat-treatment at 700–1,200 °C is in agreement with the theoretically calculated value of 0.645 cm^3/g.
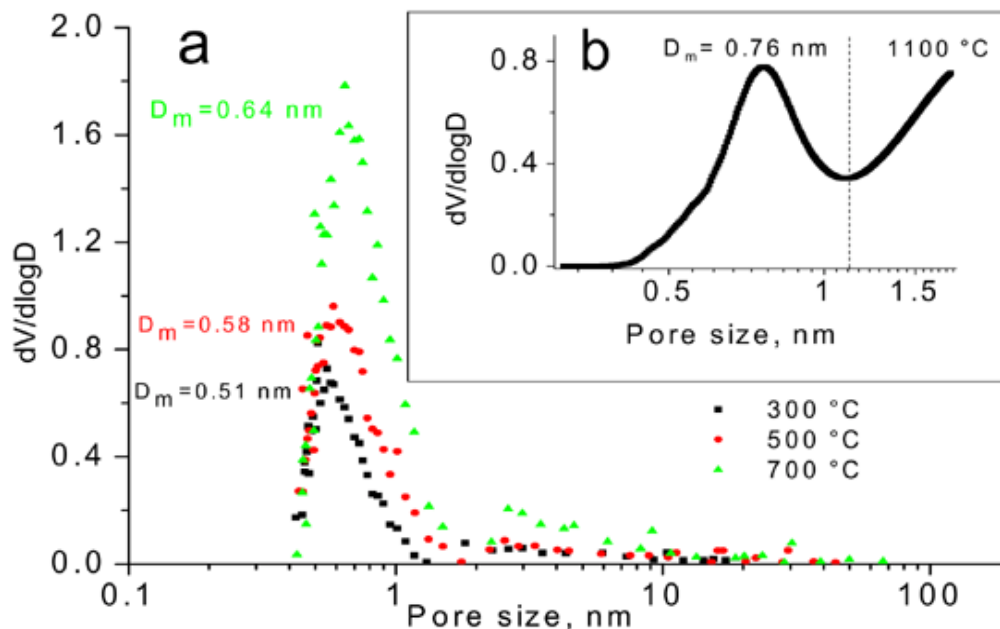
Figure 1 Differential pore-size distributions for CDC. No mesopores or macropores were detected at 300–500 °C. A small volume of mesopores of 2–4 nm in size appears at 700 °C, and the volume of mesopores increases sharply at 1,100 °C and above. Distributions were calculated assuming a slitpore model. Ar adsorption was measured at −186 °C. D_m is the pore size corresponding to the maximum in pore-size distribution.

This report summarizes our obtained results, analyses performed and conclusions reached, covering the 4 year period of the grant. Details may be found in the open literature publications listed at the end, all of which have been uploaded to the EERE Project Management website. The work is divided into 4 tasks.

Task 1: Synthesize CDC materials with greater H_2 storage capacity than known carbons

Survey experiments. Given the vast parameter space of precursor carbides, chlorine etching conditions, post-processing treatments etc., our initial strategy

was to launch in parallel a limited set of survey experimental syntheses and a modeling effort which would point the way to optimum materials based on first principles of binding, reactivity etc. We first describe the results of the survey experiments, which focus on the effects of precursor crystal structure and stoichiometry.

Here we reasoned that the larger the ratio of etchable metals/metalloids to carbon, the greater the total porosity; e.g for B_4C, complete chlorination removes 4/5 of the atoms, offering the possibility of very large internal pore volume if the structure does not collapse macroscopically upon B removal. On the other hand, since B_4C is not cubic, the local environment surrounding the remaining carbons will be rather complex, not comprised of a single C-C distance as would be expected for cubic precursors such as TiC and β-SiC. The results are shown
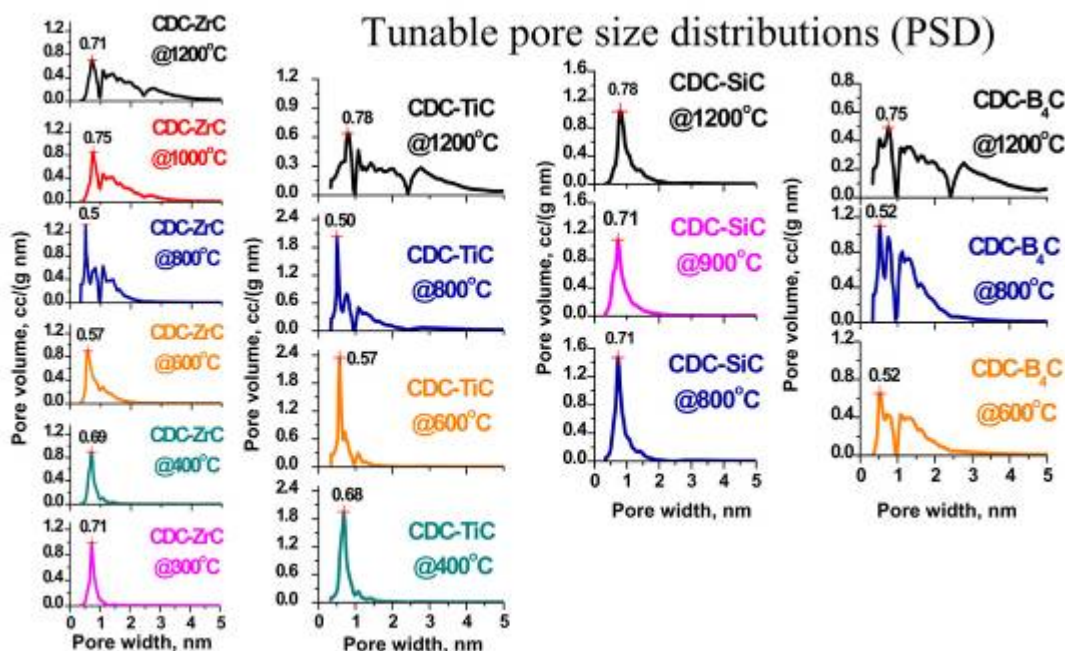
Figure 2 Differential pore-size distributions for CDCs synthesized from four different precursor carbides at 3-6 different T(Cl). In general, increasing T(Cl) leads to mesopore formation whereas at low T(Cl) all precursors except the 4:1 B_4C are dominated by micropores < 1 nm.

in Figure 2 as a 2 x 2 array of PSDs for different T(Cl) values (y-axis) and precursor carbides (x-axis). Clearly the simple picture of independent parameters is incorrect. For example SiC and TiC are isostructural, yet SiC survives as a monodisperse microporous PSD to much higher T(Cl). On the other hand, the non-cubic, metalloid-rich B_4C yields CDCs dominated by mesopores over the whole range of T(Cl) explored. Our survey included > 40 combinations of precursor carbide and chlorination temperatures. For all these

materials, hydrogen isotherms at 77 K up to 1 atm. yielded gravimetric storage capacities mostly less than 2 wt.%, well below the 2005 DOE materials target.

Modeling. Ideally we had hoped to model the chlorination process in order to "watch" the response of the system to changes in processing conditions, The major hurdle was limited knowledge of where to place the carbons in the final disordered CDC structure. The local bonding was proved by several experiments to be essentially sp^2, i.e. 3 co-planar first neighbors at 0.141 nm. X-ray diffraction established the absence of long-range order. "Solving" the amorphous structure was clearly going to be a project in itself. Thus we decided to redirect the modeling efforts to atom-scale additives, or catalysts (as described below) and to seek collaborations with experts in the experimental and theoretical aspects of radial distribution function analysis. This consists of measuring a scattering profile over a wide range of $Q = 4\pi\sin\theta/\lambda$ using x-rays or neutrons, then performing a Fourier transform to obtain $\rho(r)$, the probability of finding an atom r distance away from an identical atom at r = 0. This completely specifies the local structure, from first coordination shell to as far in real space as atom-atom correlations persist in a particular noncrystalline substance. We will present some results in a later section.

Annealing. CDC synthesis can leave behind significant amounts of metals, chlorine, chlorides and unreacted carbides, especially at low T(Cl). This degrades gravimetric capacity because a) its presence can block H2 access to some of the internal porosity, and b) it adds useless mass to the denominator in wt.%. All these impurities can be removed by annealing in flowing H_2 or NH_3, After systematically optimizing the annealing protocol, it was incorporated into the chlorination process in-line to avoid transferring samples from one furnace to another. This was the first of many post-processing attempts to get closer to DOE targets. We show here a few examples.

Figure 3 (left) shows a 17.5% reduction in Cl_2 to below 1 wt.% after 90 minutes at H_2 annealing temperatures in the range 600 – 800 ^{o}C, for a TiC-CDC resulting from chlorination at 600 ^{o}C. In this example the complete process can be done at a single temperature. Figure 3 (right) indicates an increase in total accessible pore volume after 90 minutes in NH_3 at 500 ^{o}C, which we attribute to the opening of pores previously clogged by one of the impurities mentioned above.
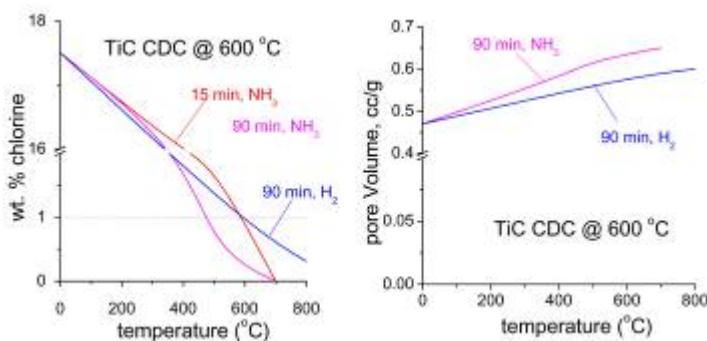
Figure 3. (left) Weight loss vs annealing temperature for TiC-CDCs annealed in H_2 or NH_3. (right) Enhanced pore volume resulting from H_2 or NH_3 annealing.

Activation. An extensive literature exists on "activation" of porous carbons by heat treating as-produced material in hot CO_2, KOH molten salt or aqueous solution. We applied the first to to CDCs as another post-processing step for enhancing hydrogen storage. The molten KOH treatments were carried out at Alicante University.

Figure 4 (left) shows the effect of hot KOH activation on specific surface area (SSA) of TiC-CDCs synthesized at T(Cl) from 400 to 1000 ^{o}C followed by annealing in H_2. This sequence has been shown to remove residual Cl and carbides first (anneal), then to chemically react with weakly bonded carbon which limits the effectiveness of pores in adsorbing hydrogen. The data show that activation is effective for any chlorination temperature, increasing the SSA by up to a factor 2, yielding 70-80% porosity. The decrease in SSA at T(Cl) = 1000 ^{o}C results from the onset of graphitization independent of activation. KOH activation increases pore volume preferentially via micropores at low chlorination temperatures. PSD's (not shown) reveal that KOH also increases the volume of larger pores as well as the average pore size.
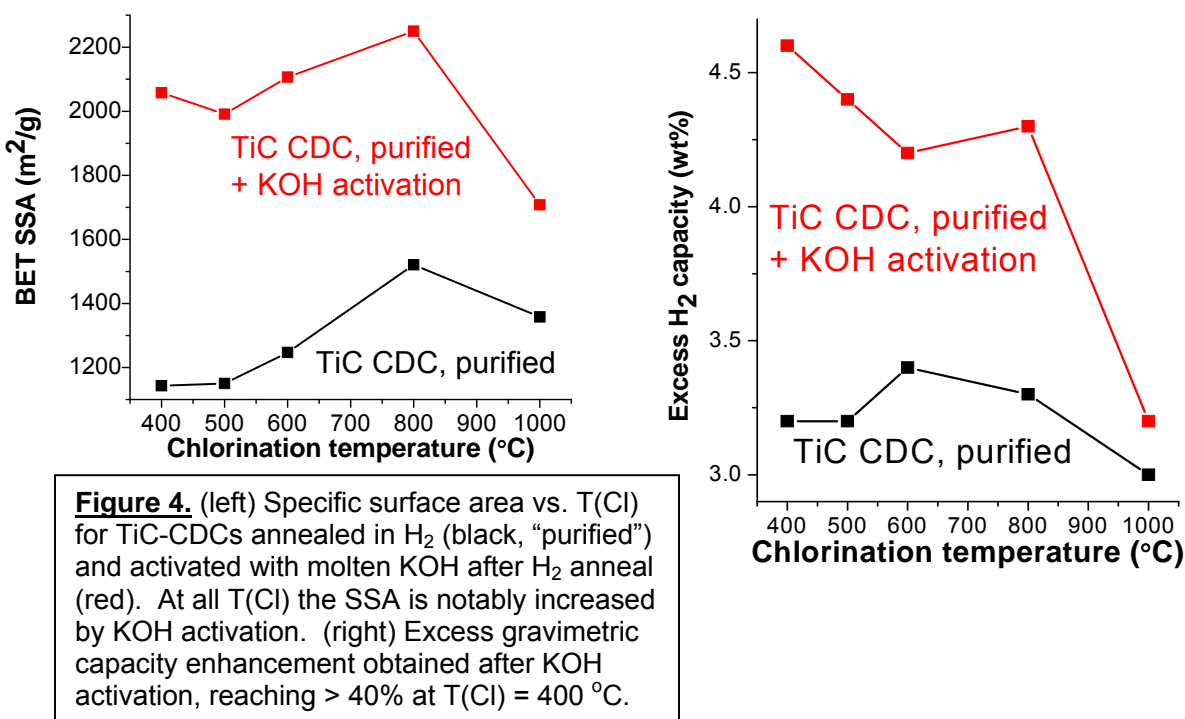

Figure 4. (left) Specific surface area vs. T(Cl) for TiC-CDCs annealed in H_2 (black, "purified") and activated with molten KOH after H_2 anneal (red). At all T(Cl) the SSA is notably increased by KOH activation. (right) Excess gravimetric capacity enhancement obtained after KOH activation, reaching > 40% at T(Cl) = 400 ^{o}C.

Figure 4 (right) shows enhanced gravimetric storage at -196 ^{o}C and 50 bar pressure resulting from KOH activation, the best result being obtained at the lowest T(Cl). Detailed PSDs (not shown) reveal that the SSA enhancement in Figure 4 (left) is primarily due to increased mesopore volume, d > 1.5 nm, which is sub-optimal for hydrogen storage. The higher T(Cl), the more dominant the macropores compared to micropores after activation. This explains why most activated carbons are not outstanding performers for hydrogen sorption; the

average pore size is too large, and too much of the porosity is accounted for by less effective pores in which adsorbed H_2 is not well-confined.

Without activation, purified SiC-CDCs underperform their TiC counterparts [2] because the volume of pores < 1 nm is smaller. Optimized CO_2 activation brings SiC-CDC performance into the range of activated TiC-CDC. Indeed the "bottom line" for activated CDCs is that as-grown low capacity materials can be brought up to the levels of the best performers, but there seems to be a fundamental limit which cannot be breached by any of the post-treatments described so far.

Volumetric capacity enhancement. DOE targets include values for volumetric capacity. Many candidate storage materials are powders of various grain sizes and ill-defined density. Thus, in parallel with our efforts to obtain higher gravimetric densities, we began to explore strategies for minimizing the inevitable volumetric penalties associated with powder materials. The first consisted of rolling peels or pressing pellets, similar to the manufacture of battery and supercapacitor electrodes from powdered materials. The second consisted of direct conversion of fully dense carbide ceramics to mononlithic CDCs.

CDC peels were rolled from a 60 wt% solution of PTFE and CDC powder suspended in ethanol, first stirred and heated to 80°C affording a putty-like substance. Self-supporting foils 0.2 – 0.4 mm thick were obtained after several passes and then dried at 100°C. Pellets ~ 5 mm diameter and 5-10 mm thick were made from the same mixture using a 5 ton hydraulic press. Density trends for two CDCs and an activated carbon are shown in Figure 5. For TiC-CDC peels we obtain a doubling of the macroscopic density, while pelletizing gives only slightly better results.
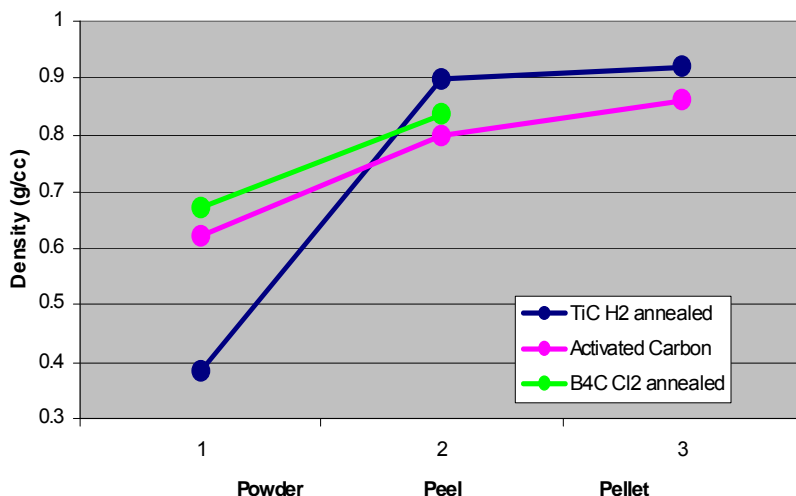

Figure 5. Schematic chart of physical densities for CDC powder, rolled peels and pressed pellets. CDC precursors are TiC (blue) and B_4C (green). Results for an activated carbon (pink) are included for comparison.

We were concerned that the mechanical forces associated with rolling or pressing might adversely affect access to the pores, or even collapse some of

them.   To quantify such effects we performed comparative H_2 Sieverts measurements at 77 K up to 60 bar H2 pressure. The results are shown in Figure 6. For SiC-CDC powder (black curve) the saturation gravimetric capacity is ~ 3.3 wt%, while after peel rolling red) it decreases to 2.5%, a rather severe 33% loss.   TiC-CDC powder is more tolerant of the mechanical abuse, decreasing by ~10% from 3.5% (green) to 3.1% (blue), a small price to pay for a doubling of the volumetric capacity.

We believe these results can be applied to similar powdered materials, certainly to other forms of amorphous carbon and possibly to MOFs and other candidate cryosorbers.
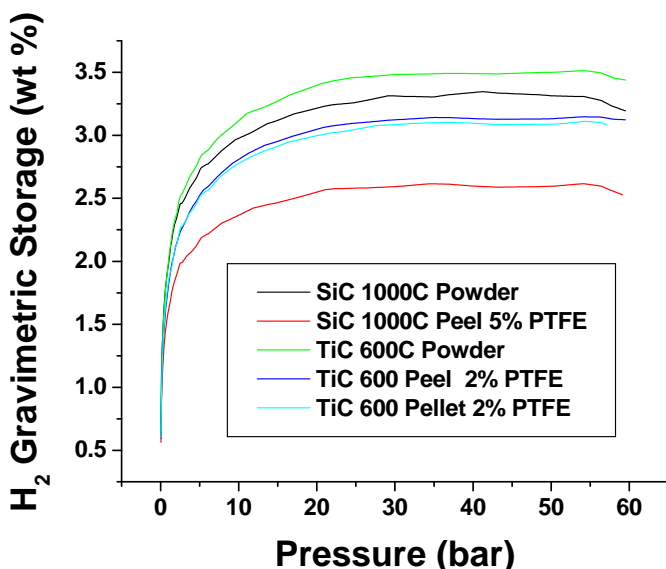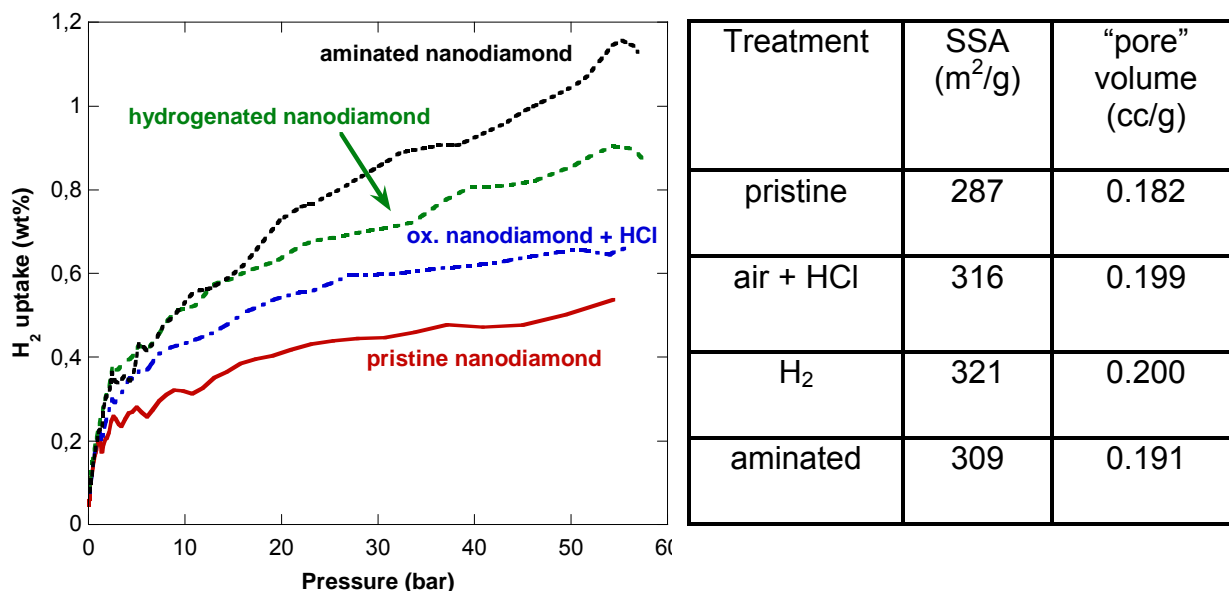

Figure 6. 77 K Sieverts measurements of excess gravimetric capacity vs. hydrogen pressure, comparing the effects of peel rolling and pellet pressing relative to powdered SiC- and TiC-based CDCs. SiC-CDC powder suffers a 33% loss after peel rolling (red vs. black curves) while for TiC the loss is only 10%. This is more than offset by the gain in volumetric capacity of ~100%.

Results from ceramic monoliths are similarly encouraging.   Densities after chlorination indicate complete removal of Ti (or Si), indicating the absence of kinetic limitations on a few mm length scale and ~hours time scale at temperatures in the 800K range.

"Pore" surface treatments. Having failed to achieve a breakthrough in pore volume while maintaining the optimum pore size distribution, we turned to modifications which would affect the pore surface chemistry, in particular by enhancing the enthalpy of adsorption on the internal surfaces. To amplify the surface effect we chose nanodiamond powders with large external surface area due to the very small ~ 5 nm particle size and no internal porosity [3]. 77 K

Sieverts data were obtained for oxidized, hydrogenated and aminated samples and compared with an untreated control sample. The results are shown in Fig. 7

Treatment	SSA (m^2/g)	"pore" volume (cc/g)
pristine	287	0.182
air + HCl	316	0.199
H_2	321	0.200
aminated	309	0.191

Figure 7 (left) and Table I (right). 77 K Sieverts isotherms of excess gravimetric capacity vs. hydrogen pressure for ~ 5 nm nanodiamond powder (control), and the same with different surface treatments. Amination of the mostly sp^3 nanodiamond leads to more than doubling of the storage capacity. Table I shows that this enhancement must be an effect of surface chemistry since the specific surface area is largely unaffected.

and in Table I. As expected, the gravimetric uptake is very small compared to CDCs, but the effect of different surface treatments is dramatic. At our maximum Sieverts pressure ~ 60 bar, the aminated sample stores more than twice the H_2 as the pristine one, with intermediate gains for oxidation and hydrogen surface termination. Table I shows that this is entirely an effect of surface chemistry, since the SSA and total "pore" volumes (actually the volume associated with the SSA assuming the surface density of C atoms) are essentially unaffected.

We note that in this surrogate experiment the surfaces are completely accessible,   albeit with small SSA. Furthermore, it is not clear that the same gains would be achieved on the primarily sp^2-coordinated CDC internal surfaces.

Precursor morphology. Synthesis of carbon by extraction of metals from carbides has been successfully used to produce a variety of microporous carbide-derived carbons (CDC) with narrow pore size distributions and tunable sorption properties. This approach is of limited use when larger mesopores are targeted, however, because the relevant synthesis conditions yield broad pore size distributions. The etching of polymer-derived ceramics allows synthesis of porous materials with a very high specific surface area and a large volume of

mesopores with well controlled size, which are suitable for applications as sorbents for proteins or large drug molecules, and supports for metal catalyst nanoparticles. In collaboration with chemists at the University of Padova, we demonstrated porosity control in the 3-10 nm range by employing preceramic polymer-derived silicon carbonitride (SiCN) precursors. Polymer pyrolysis in the temperature range 600 to 1400 °C prior to chlorine etching yields disordered or graphitic CDC materials with surface area in the range 800 to 2400 m^2/g. In the hierarchical pore structure formed by etching SiCN ceramics, the mesopores originate from etching silicon nitride (Si_3N_4) nano-sized crystals or amorphous Si-N domains, while the micropores come from SiC domains.

The reaction scheme to produce the preceramic polymer is shown in Figure 8. The resulting material can be molded, rolled or pressed into near-final shape, and then pyrolyzed at 900 – 1200 °C to afford a near-fully dense solid carbide suitable for chlorination to further afford a CDC. Modifications or combinations of silazane precursors opens the way to numerous ceramic "alloys" with controlled C/N ratios, incorporation of a third element, etc.
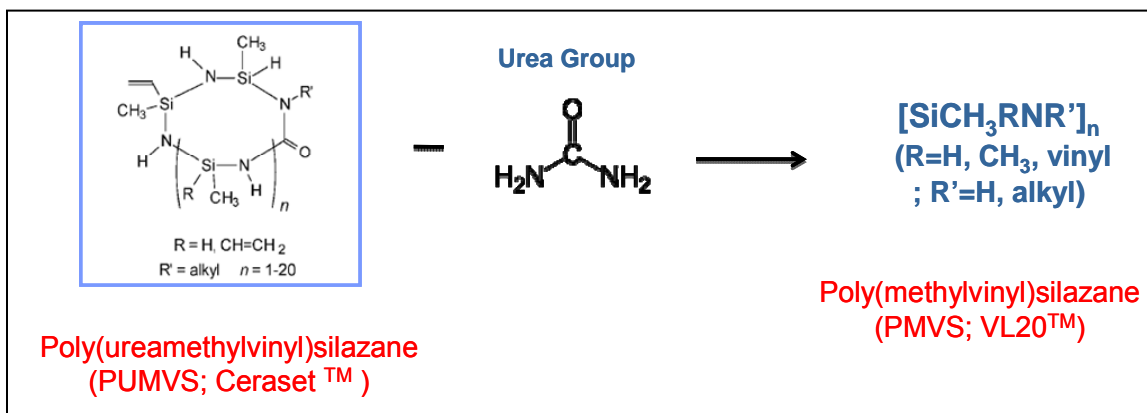
Figure 8. Reaction scheme leading to the preceramic polymer of controlled C/N ratio which is then pyrolyzed to a pure SiCN ceramic. This product then affords a new family of CDC precursors of controlled composition and morphology.

CDCs from SiCN ceramics (SiCN-CDCs) were produced by chlorination at 900 or 1200 °C. Si and N are eliminated as $SiCl_4$ and N_2, leaving behind a nanoporous network of > 98% pure carbon. Incomplete chlorination occurs at 600 and 800 °C. Two types of etching reactions occur, depending on the microstructure of the SiCN ceramics, which in turn is controlled by pyrolysis temperature. At 600 to 1200 °C, pyrolysis of amorphous SiCN occurs via the decomposition reaction $2SiC_xN_y + 4Cl_2(g) \rightarrow 2SiCl_4 (g) + yN_2(g) + 2xC(s)$, while in the SiC/$Si_3N_4$ nano-composite pyrolyzed at 1400 °C, the following reactions occur instead: $SiC + 2Cl_2(g) \rightarrow SiCl_4(g) + C(s)$ and $Si_3N_4 + 6Cl_2(g) \rightarrow 3SiCl_4(g) + 2N_2(g)$. In both cases Si and N are leached out, and C atoms self-organize into an amorphous or disordered, mainly sp2-bonded, structure. The characteristics of the mesoporosity can be controlled by varying the pyrolysis temperature, as this

affects the microstructure of the ceramic material at the nano-scale. In the etching reaction of the nanocomposite pyrolysis products, SiC leaves behind carbon atoms, and Si_3N_4 completely disappears, giving rise to the formation of larger pores (mesopores) and higher pore volumes.
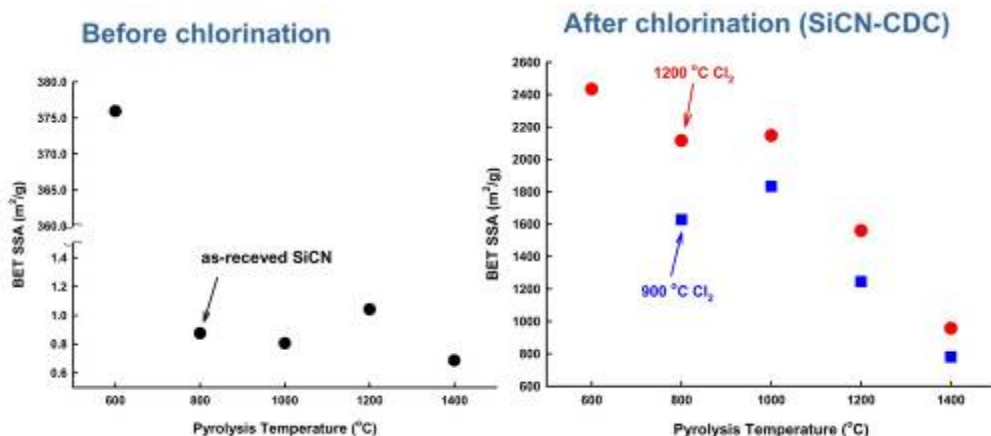
Figure 9. SSA vs. preceramic pyrolysis temperature for neat SiCN (left) and the CDC products resulting from chlorination at 900 (blue) and 1200 °C (red).

Figure 9 shows the develement of internal surface area associated with pore formation after chlorine etching. The best result is obtained by pyrolyzing SiCN at 600 °C and chlorinating the resulting ceramic at 1200 °C, namely 2400 m^2/g.

Task 2: Determine the nature and strength of H-C interactions
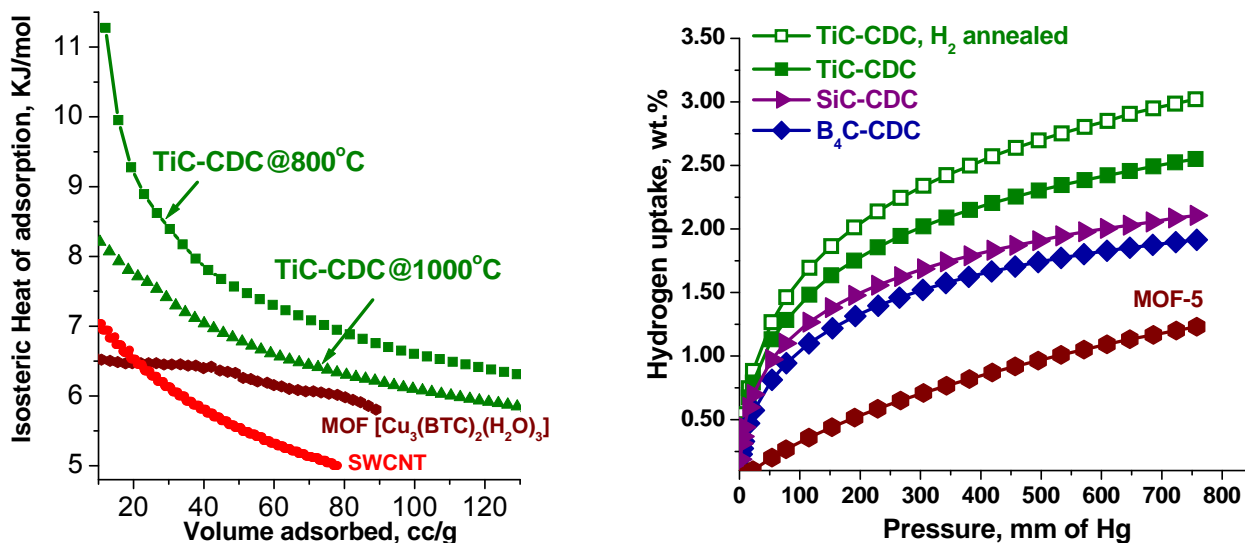

Figure 10. (left) Comparison of adsorption enthalpies for CDCs, MOF-5 and single-wall carbon nanotubes. (right) 77 K H_2 uptakes of typical CDCs compared with that of MOF-5.

Figure 10 nicely explains why CDCs outperform the early MOFs and especially carbon nanotubes with respect to hydrogen storage. On the left panel we plot

the coverage-dependent adsorption energies for TiC-CDCs chlorinated at 800 and 1000 ^oC, the metal-oxide framework compound MOF-5, and a sample of single-walled carbon nanotubes. Here the isosteric (constant volume) heat of adsorption is derived via the Clausius-Clapeyron equation from hydrogen isotherms at 77 K and 88 K corresponging to the boiling points of N_2 and Ar respectively. For reference the low-coverage value for graphite is ~5 KJ/mole. The right panel of Fig. 10 compares excess gravimetric capacities of typical CDCs with that of MOF-5. Note that the maximum pressure is only 1 bar; this data was obtained before we built our high pressure Sieverts apparatus. It is significant that both the hydrogen-annealed CDC and MOF-5 are not saturated, thus the capacities will continue to increase with pressure above 1 bar; indeed the TiC-CDC reaches 4.5 wt% at 50 bar. Clearly high heat of adsorption is the key to further improvements in storage capacity.

A related approach to modifying the interaction strength between molecular hydrogen and porous carbons is to introduce "catalytic" metal centers consisting of rehybridized metal valence orbitals and bonding orbitals of the extended π system characteristic of graphene. Early reports of success with alkali metal doping turned out to be due to oxygen and water contamination. A well-known phenomenon from organometallic chemistry is the so-called Kubas interaction [4], whereby the d-levels in a light transition metal form a partly-filled hybrid orbital with the carbon π system, which then can bind H_2 with enthalpies intermediate between physic- and chemisorption. Calculations were performed on H_2-decorated Ti-C complexes based on simple surrogates for pores in amorphous carbon, in particular the C_{60} molecule [5]. Only absolute minima in the free energy were identified; none of these corresponded to the desired configuration, which was thus claimed to be unstable. Our theory group at NIST took a broader approach, allowing metastable states which would be substantially populated and essentially stable on any practical time scale. Some
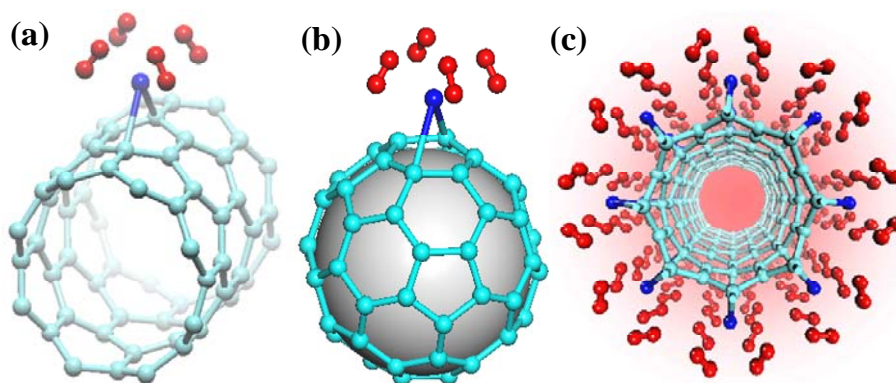
Figure 11. Carbon structures (light blue) to which Ti (dark blue) is bonded via Kubas hybridization. a) one Ti on an 8,0 nanotube. b) one Ti on a C_{60} molecule. c) maximum packing of Ti on the nanotube. In all 3, each Ti can bind 4 H_2's via Kubas hybridization. The latter corresponds to 8 wt% H_2, including Ti and C in the total weight.

of the resulting structures are shown in Figure 11 below [6]. In a) we see a single Ti atom (dark blue) bridging a carbon hexagon (light blue) in a nanotube, to which is bound a maximum of 4 H_2 molecules. In b) we have the same situation on a C_{60} molecule. In c) we return to the nanotube, decorated with the maximum surface density of Ti's, each of which can still bind 4 H_2's. For an (8,0) nanotube this corresponds to 8 wt% hydrogen.

Most recently, we found to our surprise that the interaction of Ti with the C=C double bond of ethylene C_2H_4 mimics what we found in C_{60}. Detailed first-principles calculations [6c] show that the complex resulting from attaching a Ti atom to each ends of C_2H_4 (Figure 12) will reversibly adsorb ten H_2 molecules. The equivalent material gravimetric capacity of 14%, if realized in practice, would readily exceed the 2015 DOE system goal.
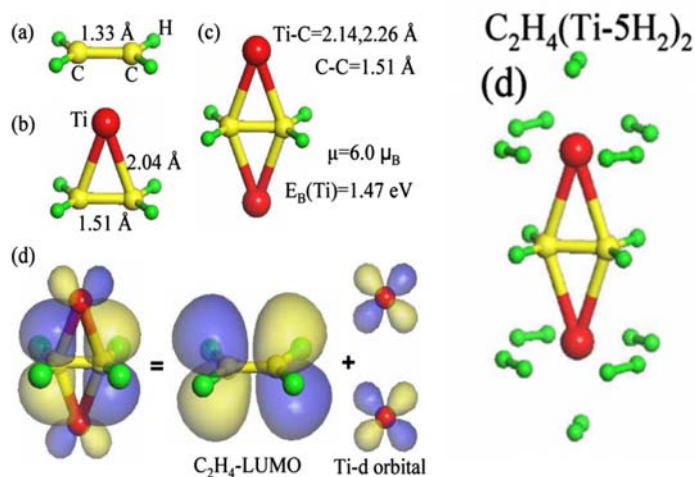
Figure 12. Kubas interaction on the ethylene molecule (a). Here the colors are yellow (carbon), red (Ti) and green (H_2). Ti can bind to one (b) or both (c) sides of C_2H_4. The partly-filled Kubas orbital is shown on the far left as a hybrid of the C_2H_4 LUMO and the Ti d-orbital (d). The cartoon on the far right shows 6 H2's plus the original 2 from ethylene bonded to the Kubas moiety. The binding energy is 0.24 eV/H_2, or ~9kT at room temperature, and the equivalent gravimetric capacity is 14%.

We immediately began experiments to incorporate atomically-divided Ti atoms into the CDC material, hopefully somewhere near the pores. Purposely leaving behind some Ti after production of TiC-CDC was an obvious strategy that didn't work; hydrogen capacity was severely degraded, possibly because the weight penalty was too high but more probably because the Ti was not optimally located in the CDC. Several attempts were made by bubbling $TiCl_4$ through the chlorination chamber, but due to the high temperatures involved we invariably obtained Ti nanoclusters, shown in Figure 13 below.
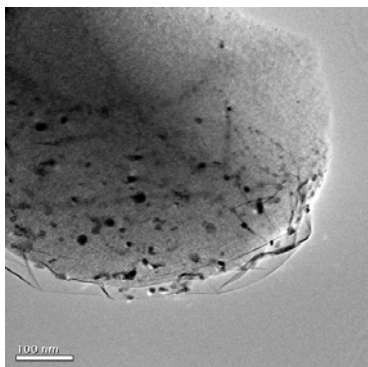


Figure 13. High resolution transmission electron microscope image of a Mo_2C-CDC particle exposed to decomposing $TiCl_4$ at 900 °C. Scale bar 100 nm. The black particles were identified as Ti by energy-dispersive x-ray spectroscopy.

Ti was introduced as $TiCl_4$ by passing Ar over a bubbler at 26-85°C and then reacted at 250°C followed by a second H_2 anneal at 400°C to remove chlorine. The aggressive $TiCl_4$ conditions reduced the *apparent* capacity by ~30%. Changes in all properties were insignificant using milder conditions. The program ended before we could quantitate the Ti, determine pore volume and find out if indeed the heat of adsorption was affected in any way. Further work is needed to optimize the Ti environment and confirm atomic level dispersion.
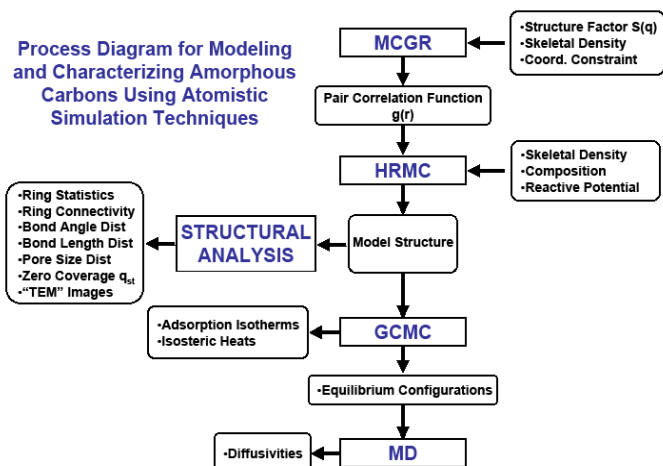
A group of catalysis scientists at the University of Virginia noticed our publication on ethylene complexes, and proceeded to design an experiment to test the idea [7]. Using laser ablation they deposited an ultrathin film of Ti, in an ethylene environment, onto an acoustic wave microbalance. After long exposure to H_2 at 1 bar pressure, they observed 14 % weight uptake, precisely what we predicted for isolated ethylene molecules. Furthermore, replacing H_2 with D_2 nicely gave twice the weight gain. While there is absolutely no proof that the active species in their chamber is $C_2H_4(Ti - 5H_2)_2$, Figure 12, the weight gain values (Figure 14 below) are strongly suggestive.
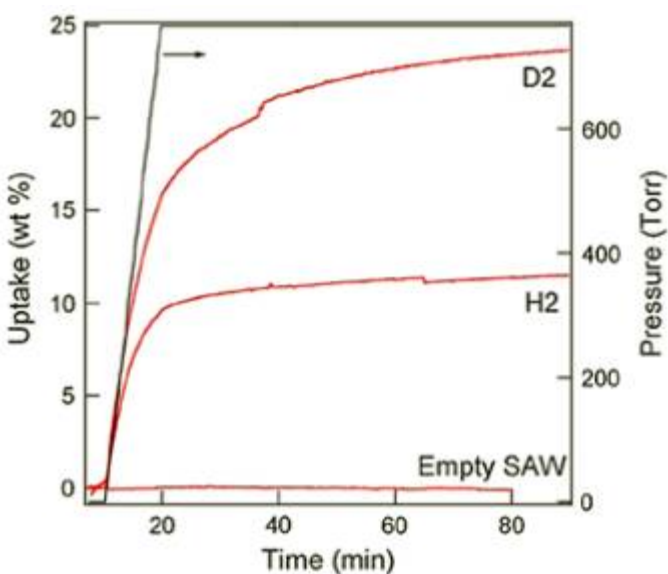
Figure 14. Molecular hydrogen weight uptake vs time of thin films deposited by laser ablation of Ti in C_2H_4 atmosphere onto an acoustic wave microbalance (PRL**100**, 105505 (2008). The film is presumed to be $C_2H_4Ti_2$ as in Fig. 12c). Exposure to H2 or D2 leads to 14% or 28% weight gain upon saturation at 1 bar.

In principle sorbate-sorbent energetics are also accessible to direct quantum chemical modeling if the C and H_2 positions are known over a reasonable length scale. This is the approach taken in our collaboration with Los Alamos National Lab and Prof. K. Gubbins' group at North Carolina State University. The overall strategy and task map is shown schematically in Figure 15 below. We described earlier the process by which the pair correlation function g(r) is obtained by Fourier transforming the experimental structure function S(Q) determined from x-ray or neutron scattering. This is least-squares-fit to a model g(r) consisting of a sequence of Gaussians representing near-neighbor correlations extending as far in real space as necessary to represent correctly the short-range order in a glassy or amorphous material. In Gubbins' version, realistic interparticle

energies are added as constraints on g(r), referred to as the hybrid reverse Monte Carlo (HRMC) method. Once the model structure is obtained accurately,

Figure 15. Flow chart of the HRMC method for studying bonding energetics in sorbate-sorbent systems. The input is a hypothetical pair correlation function determined by Monte Carlo methods (MCGR). This is optimized with respect to the measured g(r) to determine a set of ~800 atomic coordinates which define the pore structure

adsorption isotherms and isosteric heats of adsorption and desorption can be calculated using Grand Canonical Monte Carlo (GCMC) methods. Preliminary results comparing the properties of TiC-CDC @ 800 ^{o}C with those of a commercial ultramicroporous carbon have been presented at several conferences and published in a Proceedings volume. This work is continuing beyond the end of the EERE grant with the ongoing participation of Los Alamos and University of North Carolina.
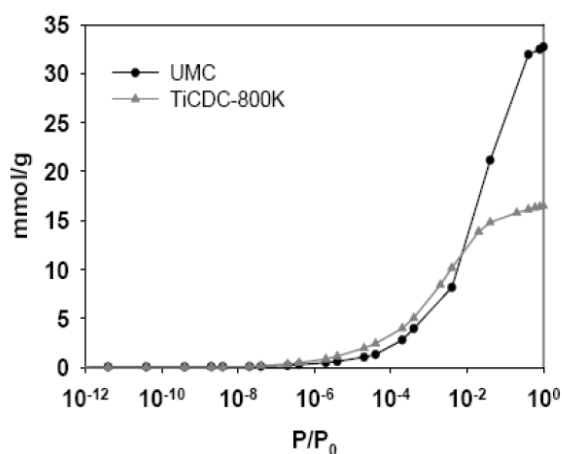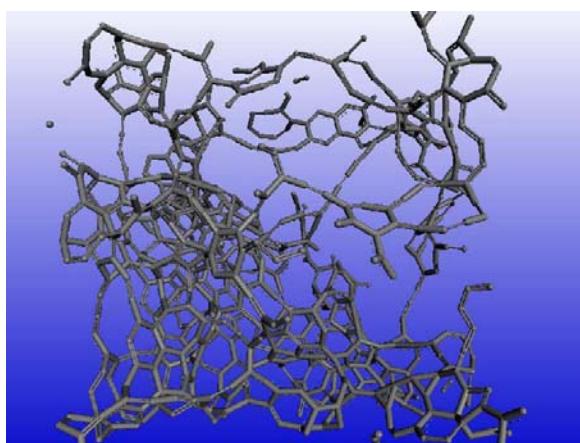
Figure 5: *Adsorptions isotherms for argon at 77K*

Figure 16. (left) optimized carbon positions for an 800 atom system with a density corresponding to TiC-CDC @ 800 ^{o}C. Bonds are drawn between atom pairs closer than 0.16 nm. The simulation box is barely large enough to reveal portions of 2 or 3 micropores. (right) Comparison of Ar adsorption isotherms for a commercial ultramicroporous carbon and a CDC.

Task 3. Determine correlation of pore size and monodispersity with H capacity and kinetics

Molecular hydrogen adsorption data for a wide range of activated carbons depend linearly on total surface area, or SSA, suggesting that the size, size distribution, pore surface chemistry etc. are either identical or not important. This gave rise to the "Chahine Rule": 1 wt% storage per 500 m^2/gm SSA [8]. Both scenarios are unlikely given the diverse precursors, processing conditions and activation chemistries employed. Having accumulated a large database of CDC adsorption data, we introduced a new kind of plot consisting of gravimetric capacity normalized to specific TOTAL pore surface area (SSA) vs. the average pore size. The Chahine Rule implies that there would be no discernible correlations in such a plot. What we found instead was a scatter plot with all data points lying within a well-defined triangular region, Figure 17, showing a definite "overperformance" for materials with small average pore sizes. This indicates
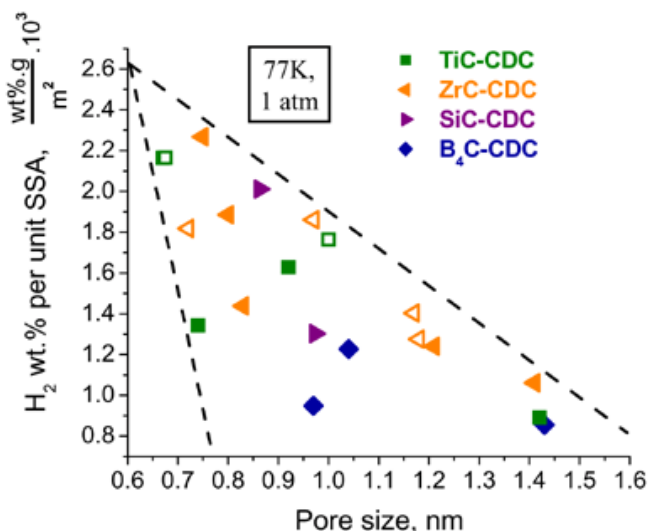
Figure 17. Modified Chahine Rule plot in which gravimetric capacity is normalized to SSA and the independent variable is average pore size rather than SSA. There is a clear trend indicating that small micropores are more efficient at sorbing molecular hydrogen than larger mesopores.

that subnanometer pores are more efficient than larger ones for H_2 adsorption on carbon surfaces. We know from PSD measurements that subnanometer pores are obtained from fcc TiC and ZrC (green and orange symbols respectively), while B_4C (blue) gives larger pores. Extrapolating the dashed lines delineating the accessible materials suggests that a SSA of ~2600 m^2/g dominated by pores of order 0.6 nm diameter would afford 6 wt% at 1 atm. and 77K. CDC with 0.92 cm^3/g pore volume (67% porosity) gives 4.5 wt.% H_2 storage if all pores are < 1 nm, even at 1 atm. where all the pores are not filled. Larger pores are detrimental to volumetric capacity since they contribute empty volume without efficiently adsorbing hydrogen. As shown previously, annealing in hydrogen (open symbols) removes residual Cl_2, increasing the pore volume available for storage.

Another way to present the data is to divide the traditional Chahine plot into two separate graphs, one each for total pore volume (or SSA) accounted for by sub-nm and super-nm pores, as show below in Figure 18. Accounting exclusively for sub-nm pores, a strong linear correlation between gravimetric capacity and pore volume is indeed observed. The hypothetical blue line assumes that all nanopores comprised in a given volume are filled with H_2, in which case a gravimetric capacity in excess of 4.5% would be achieved at 1 atm. and 77 K with a narrow distribution of 0.6 nm pores. The ternary precursor Ti_3SiC_2 yielded CDCs which already met these pore specifications before this project began, but the 1 atm. 77 k capacity was only 2-3% indicating that only a fraction of the micropores was capable of adsorbing hydrogen.
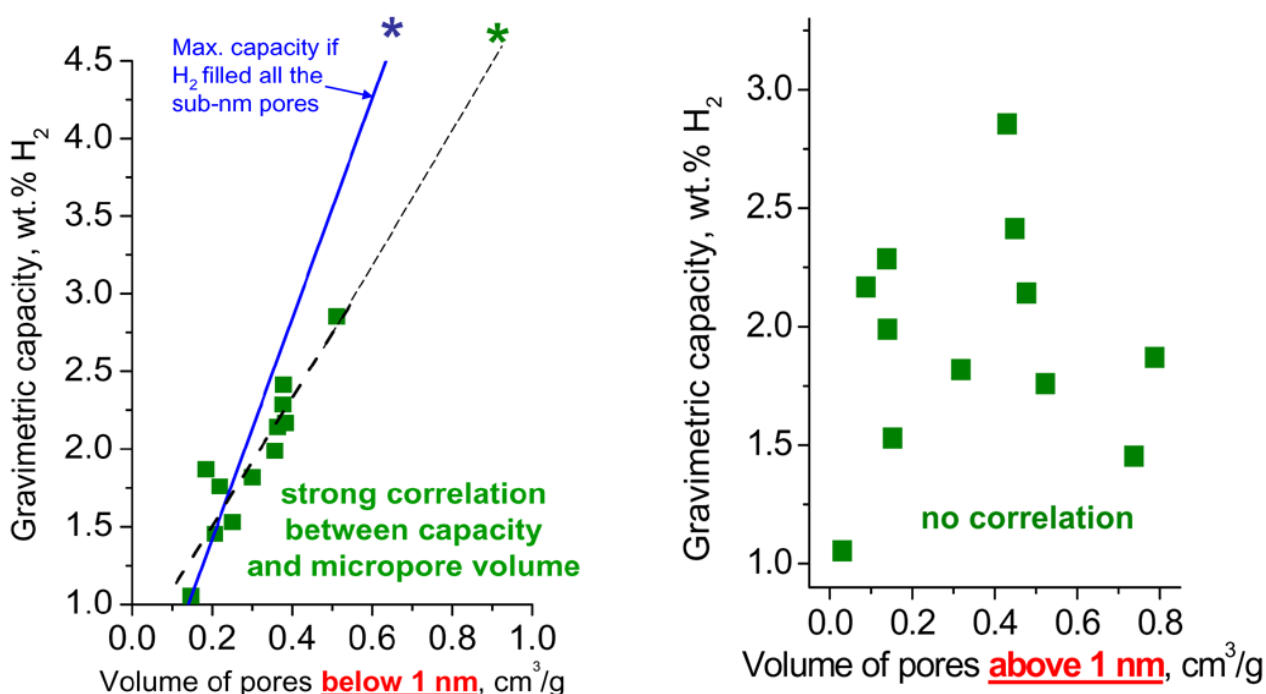
Figure 18. Correlations between gravimetric capacity and pore volumes < 1nm (left) and > 1m (right). The former gives a strong linear correlation analogous to the Chahine Rule, while the latter appears totally random.

Task 4. Identify optimum carbon, demonstrate scale-up, find industrial partner and commercialize

We consistently found that TiC-CDC with T(Cl) = 800 ^{o}C gave the highest gravimetric excess capacity, on average 4.3% at 77 K and 60 atm. One data set using Mo_2C gave comparable results. Unfortunately SiC, one of the least expensive carbides, did not provide the highest capacity.

Typical batch size for these experiments was 300 mg. We attempted to scale up using a fluidized bed, but failed to achieve sufficient uniformity. With help from colleagues in Europe we found that simply scaling up to a larger tube furnace and quartz boat to contain the powder, the batch size could be increased by 4X. Coupled with in-line annealing and/or activation and higher chlorine flow rates, kilos per day can be produced.

Several local firms were approached with offers to jointly engineer a scaled-up manufacturing capability, to no avail. Prof. Gogotsi and his Drexel colleagues proceeded to create a start-up named Y-Carbon [9], which has obtained sufficient venture capital to occupy 1600 sq. feet of lab and office space nearby in King of Prussia. They recently hired a CEO and are currently seeking to add technical staff.   They also seek partnerships to develop CDCs for a wide variety of applications.

OUTLOOK AND PROSPECTS

After 5 years of research and participation in the EERE hydrogen program, the PI's agree that porous carbons offer little promise for on-board hydrogen storage under practical conditions of temperature and pressure. Three "show-stoppers" are readily identified:

1. Despite achieving SSAs approaching 4000 m^2/g in some cases, the concomitant storage is far below the Chahine Rule "prediction" of 8 wt% since only a fraction of the pores are small enough to bind H_2,

2. Even with large micropore volume, the binding enthalpies are too weak to permit operation at reasonable temperatures and pressures. There do not appear to be any kinetic issues, as evidenced by complete conversion from carbide to carbon starting with micron-size powders or ~mm thick ceramic monoliths. The modest binding energies imply that issues of heat

rejection during cycling will be no more severe than in similar porous carbons

3. To the best of our knowledge none of the experimental work on any porous carbon includes a consideration of the thermodynamics of adsorption and desorption [10]. Under practical cycling conditions not all of the adsorbed hydrogen can be recovered and burned, adding yet another weight and volume penalty on the capacity targets.

4. Further BES-level work on atomic-scale Ti doping would make sense if the transition metal-ethylene complex in Ref. [5] is ultimately identified as a likely configuration in Ti-doped sp2 carbon.

As noted at the beginning of this report, there are many other applications for which CDCs are well-suited. A biomedical company in England is developing CDCs for the health care industry. Electrochemical energy storage looks very promising. In both fields, the original finding of tuneable pore size over a wide range [1] is the key property of interest.

References

[1] Nanoporous Carbide-derived Carbons with Tuneable Pore Size, Y. Gogotsi, A. Nikitin, H. Ye, W. Zhou, J. E. Fischer, B. Ye, H. Foley and M. Barsoum, *Nature Materials* **2,** 591 (2003).

[2] Design of Porous Carbon for Efficient Hydrogen Storage, G. Yushin, R.K. Dash, J. Jagiello, J. E. Fischer, Y. Gogotsi, *Adv. Funct. Mat.* **16**, 2288-2293 (2006).

[3] Control of sp2/sp3 Carbon Ratio and Surface Chemistry of Nanodiamond Powders by Selective Oxidation in Air, S. Osswald, G.Yushin, V. Mochalin,.S.O. Kucheyev and Y. Gogotsi, *J. Am. Chem. Soc.* **128**, 11635-11642 (2006).

[4] Metal Dihydrogen and Bond Complexes - Structure, Theory and Reactivity, edited by G. J. Kubas (*Kluwer Academic/Plenum Publishing, New York* 2001).

[5] Clustering of Ti on a C_{60} Surface and Its Effect on Hydrogen Storage, Q. Sun, Q. Wang, P. Jena and Y. Kawazoe, *J. Am. Chem. Soc.* **127,** 14582-14583 1(2005).

[6a] Titanium-Decorated Carbon Nanotubes as a Potential High-Capacity Hydrogen Storage Medium, T. Yildirim and S. Ciraci, *Phys. Rev Letters* **94**, 175501 (2005).

[6b] Vibrational properties of TiH_n complexes adsorbed on carbon nanostructures, J. Iniguez, W. Zhou and T. Yildirim, *Chem Phys. Letters* **444**, 140-144 (2007).

[6c] Hydrogen absorption properties of metal-ethylene complexes, W. Zhou, T. Yildirim, E. Durgun, and S. Ciraci, *Phys. Rev. B* **76**, 085434 (2007).

[7] High Capacity Hydrogen Absorption in Transition Metal-Ethylene Complexes Observed via Nanogravimetry, A. B. Phillips and B. S. Shivaram, *Phys. Rev. Letters* **100,** 105505-105508 (2008).

[8] Modeling of adsorption storage of hydrogen on activated carbons, P. Benard and R. Chahine, *Int. J. Hydrogen Energy* **26,** 849–855 (2001).

[9] http://www.y-carbon.us/Home.aspx

[10] Optimum Conditions for Adsorptive Storage, S. K. Bhatia and A. L. Myers, *Langmuir* **22**, 1688-1700 (2006).

PATENTS and PUBLICATIONS 2005-2009

Process for producing nanoporous carbide-derived carbon with increased gas storage capability, PCT/US2006/021140.

Tailoring of nanoscale porosity in carbide-derived carbons for efficient hydrogen storage, Y. Gogotsi, R. K. Dash, G. Yushin, T. Yildirim, G. Laudisio and J. E. Fischer, *J. Am. Chem. Soc.* **127,** 16006 (2005).

Molecular and dissociative adsorption of multiple hydrogen molecules on transition metal decorated C_{60}, T. Yildirim, Jorge Iniguez, and S. Ciraci, *Phys. Rev.* **B72**, 153403 (2005).

Titanium-Decorated Carbon Nanotubes as a Potential High-Capacity Hydrogen Storage Medium, T. Yildirim and S. Ciraci, *Phys. Rev Letters* **94**, 175501 (2005).

Double-layer capacitance of carbide-derived carbons in sulfuric acid, J. Chmiola, G. Yushin, R. Dash, E. Hoffman, J. E. Fischer, M. Barsoum and Y. Gogotsi, *Electrochem. and Solid State Letters* **8,** A357-A360 (2005).

Titanium Carbide-Derived Nanoporous Carbon for Energy-Related Applications, R.K. Dash, G. Yushin, G. Laudisio, J. Chmiola, J. E. Fischer, Y. Gogotsi, *Carbon* **44**, 2489-2497 (2006).

Design of Porous Carbon for Efficient Hydrogen Storage, G. Yushin, R.K. Dash, J. Jagiello, J. E. Fischer, Y. Gogotsi, *Adv. Funct. Mat.* **16**, 2288-2293 (2006).

Carbide-Derived Carbons: A Comparative Study of Porosity Based on Small-Angle Scattering and Adsorption Isotherms, G. Laudisio, R.K. Dash, G. Yushin, J.P. Singer, Y. Gogotsi, J.E. Fischer, *Langmuir* **22**, 8945-8950 (2006).

Vibrational properties of TiH_n complexes adsorbed on carbon nanostructures, J. Iniguez, W. Zhou and T. Yildirim, *Chem Phys. Letters* **444**, 140-144 (2007).

Hydrogen absorption properties of metal-ethylene complexes, W. Zhou, T. Yildirim, E. Durgun, and S. Ciraci, *Phys. Rev. B* **76**, 085434 (2007).

Desolvation of ions in subnanometer pores, its effect on capacitance and double-layer theory, J. Chmiola, C. Largeot, P.-L. Taberna, P. Simon, Y. Gogotsi, *Angewandte Chemie Int. Edition* **47** (18), 3392-3395 (2008).

Relation between the Ion Size and Pore Size for an Electric Double-Layer Capacitor, C. Largeot, C. Portet, J. Chmiola, P.L. Taberna, Y. Gogotsi, P. Simon, *J. Am. Chem. Soc.* **130** (9), 2730-2731 (2008)

Enhanced volumetric hydrogen storage capacity of porous carbon powders by forming peels or pellets, J. P. Singer, A. Mayergoyz, C. Portet, E. Schneider, Y. Gogotsi and J. E. Fischer, *Mesoporous and Microporous Materials* s **116,** 469–472 (2008).

Carbide Derived Carbon Membrane, E. N. Hoffman, G. Yushin, B. G. Wendler, M. W. Barsoum, Y. Gogotsi, *Mat. Chem. Phys.* **112**, 587-591 (2008).

Enhanced volumetric hydrogen storage capacity of porous carbon powders by forming peels or pellets, J. P. Singer, A. Mayergoyz, C. Portet, E. Schneider, Y. Gogotsi and J. E. Fischer, *Mesoporous and Microporous Materials* **116,** 469–472 (2008).

Carbide Derived Carbon and Templated Carbons, T. Kyotani, J. Chmiola, Y. Gogotsi, Chapter 3 in *Carbons and Composites for Electrochemical Energy Storage Systems,* edited by F. Beguin and E. Frackowiak, CRC Press/Taylor and Francis, pp. 77-113 (2009).

Porosity control in nanoporous carbide-derived carbon by oxidation in air and carbon dioxide, S. Osswald, C. Portet, Y. Gogotsi, G. Laudisio, J. P. Singer; J. E. Fischer, V. Sokolov, J. Kukushkina, A. Kravchik, *J. Solid State Chem.* **182**, 1733–1741 (2009).

Hybrid Reverse Monte Carlo Simulations of Nano-Porous Carbons, J.C. Palmer, S.K. Jain, K.E. Gubbins, N. Cohaut, J.E. Fischer, R.K. Dash and Y. Gogotsi, in

Characterization of Porous Solids VIII, Proceedings of the 8th International Conference on Characterization of Porous Solids, Eds. S. Kaskel, P. Llewellyn, F. Rodriguez-Reinsos and N.A. Seaton, pp. 56-63, Royal Society of Chemistry, Cambridge, Special Publication No. 318 (2009).

Molybdenum carbide-derived carbon for hydrogen storage, H. S. Kim, J. P. Singer, Y. Gogotsi and J. E. Fischer, *Mesoporous and Microporous Materials* **120**, 267-271 (2009).

Enhanced methane storage of chemically and physically activated carbide-derived carbons, S. Yeon, S. Osswald, Y. Gogotsi, J. P. Singer, J. M. Simmons, J. E. Fischer, M.A. Lillo-Rodenas, A. Linares-Solano, *J. Power Sources* **191**, 560 (2009).

Capacitance of KOH Activated Carbide-Derived Carbons, C. Portet, M.A. Lillo-Rodenas, A. Linares-Solano, Y. Gogotsi, Phys. Chem. Chem. Phys. **11,** 4943-4945 (2009)

Importance of Pore Size in High Pressure Hydrogen Storage by Porous Carbons, Y. Gogotsi, C. Portet, S. Osswald, J. Simmons, T. Yildirim, G. Laudisio, J. E. Fischer, *Int. J. Hyd. Energy* **34**, 6314-6319 (2009).

Carbide-Derived-Carbons with Hierarchical Porosity from a Preceramic Polymer, S.-H. Yeon, P. Reddington, Y. Gogotsi, J. E. Fischer, C. Vakifahmetoglu, and P. Colombo, *Carbon* **48**, 201 –210 (2010).

Modeling the structural evolution of carbide-derived carbons using quenched molecular dynamics, J. C. Palmer, A. Llobet, S.-H. Yeon, J. E. Fischer, Y. Shi, Y. Gogotsi and K. E. Gubbins, *Carbon* (2010 in press).

Enhanced volumetric hydrogen and methane storage capacity of monolithic carbide-derived carbon, Sun-Hwa Yeon, Isabel Knoke, Yury Gogotsi, John E. Fischer, *Mesoporous and Microporous Materials* (submitted).

PRESENTATIONS 2005-2009

Porous Carbide Derived Carbons (CDC) Optimized for Hydrogen Storage: a SAXS Study; G. Laudisio, R. K. Dash, J. P. Singer, G. Yushin, T. Yildirim, Y. Gogotsi, J.E. Fischer, *Fall MRS Symposium*, Boston 11-12/2005.

High Hydrogen Storage in porous Carbide Derived Carbon, G. Laudisio, T. Yildirim, R. K. Dash, G. Yushin, Y. Gogotsi, J.E. Fischer, *Fall MRS Symposium*, Boston 11-12/2005.

Nanoporous Carbide Derived Carbon with Tunable Pore Size: Synthesis and Energy-Related Applications, Gleb Yushin, John Chmiola, Ranjan K. Dash, Elisabeth Hoffman, Michel Barsoum, Yury Gogotsi,Giovanna Laudisio and <u>John E. Fischer</u>, invited lecture at the *First International Conference on Carbon for Energy Storage and Environment Protection (CESEP)*, Orleans France, October 2-6, 2005.

From fundamental understanding to predicting new nanomaterials for high capacity hydrogen storage technologies, T. Yildirim, *APS March Meeting*, Baltimore 2006.

Carbide Derived Carbon Designed for Efficient Hydrogen Storage, <u>R.K. Dash</u>, G. Yushin, G. Laudisio, T. Yildirim, J. Jagiello, J.E. Fischer and Y. Gogotsi, *Spring MRS Symposium*, San Francisco, April 2006.

Combined Neutron Scattering and First-Principles Study of Novel Hydrogen Storage Materials, T. Yildirim, *Spring MRS Symposium*, San Francisco, April 2006 (invited).

Tailored nanoscale porosity in carbide-derived carbons optimized for hydrogen storage, *John E. Fischer,* Giovanna Laudisio, Jonathan P. Singer, Ranjan K. Dash, Gleb Yushin, Yury Gogotsi, Taner Yildirim, *E-MRS Symposium E, Hydrogen Storage Materials*, Nice, France, May 2006.

Neutron Scattering and First-Principles Characterization of Novel Hydrogen Storage Materials, T. Yildirim, *American Conference on Neutron Scattering*, St. Charles, IL, June 18-22, 2006 (invited).

Magic Role of Ti in Novel Hydrogen Storage Materials, T. Yildirim, *XV International Materials Research Congress (IMRC),* Cancún, August 20–24, 2006 (invited).

Tailored nanoscale porosity in carbide-derived carbons: optimization for high capacity hydrogen storage, Yury Gogotsi et al., *UCSB Conference on Hydrogen Storage* (sponsored by DOE) August 2006.

Tailored nanoscale porosity in carbide-derived carbons: optimization for high capacity hydrogen storage, John E. Fischer, *MH2006 (Metal-Hydrogen interactions),* Maui, October 1–4, 2006 (invited).

Hydrogen and Methane in MOF - Isotherms, Heat of Absorptions and INS Data, Wei Zhou and Taner Yildirim, *MH2006 (Metal-Hydrogen interactions*), Maui, October 1–4, 2006.

Characterization of Carbide Derived Carbons (CDC) structure and its effect on hydrogen storage, J. P. Singer, G. Laudisio, A. B. Seletsky, R. K. Dash, G.

Yushin, W. Zhou, T. Yildirim, Y. Gogotsi, J.E. Fischer, *MRS Fall Meeting, Symposium Z: Hydrogen Storage Technologies,* Boston, November 27–December 1, 2006.

Carbide-derived carbons: effect of pore size on hydrogen uptake and heat of adsorption, Gleb Yushin, Ranjan K. Dash, Daniel Vriehof, Yury Gogotsi, Taner Yildirim, Giovanna Laudisio, Jonathan P. Singer, John E. Fischer, *MRS Fall Meeting, Symposium Z: Hydrogen Storage Technologies*, Boston, November 27–December 1, 2006.

Activation of Carbide Derived Carbons (CDC) for Effective Hydrogen Storage, G. Laudisio, R. K. Dash, J. P. Singer, G. Yushin, W. Zhou, T. Yildirim, Y. Gogotsi and J. E. Fischer, *MRS Fall Meeting Symposium Z: Hydrogen Storage Technologies,* Boston November 27 - December 1, 2006.

Nanotechnology in Energy Technology (invited), Y. Gogotsi, *Nanotechnology in Energy Forum organized by Ben Franklin Technology Partners of Southeastern Pennsylvania,* Penn State, November 14, 2006.

Hydrogen Absorption Properties of Metal-Ethylene Complexes, W. Zhou, and T. Yildirim, E. Durgun, S. Ciraci, NIST Sigma-Xi Postdoctoral Poster Presentation, Gaithersburg, MD. 2007.

Carbide-Derived Carbons for Energy-Related and Biomedical Applications (invited), Y. Gogotsi, *From the Lab to the Marketplace: Nanotechnology Symposium*, Polytechnic University, Brooklyn, NY, April 23, 2007.

Hybrid reverse Monte Carlo simulations of nanoporous carbons, J. Palmer, S. Jain, K. Gubbins, N. Cohaut, J. E. Fischer and Y. Gogotsi, Proceedings of the 8th International Symposium on the Characterisation of Porous Solids, Scotland (2008).

Carbide-Derived Carbons for Energy-Related Applications, Y. Gogotsi, University of Connecticut, School of Engineering, February 28, 2008.

Nanostructured Carbons and Carbon-Based Nanocomposites for Energy Related Applications, G. Yushin, *American Chemical Society 235th National Meeting*, New Orleans, Louisiana, April 2008 (invited).

Progress in Carbide-Derived Carbons for Energy Related Applications, Y. Gogotsi, keynote address at *Carbon for Energy Storage and Environment Protection (CESEP II* Sept. 2-6, 2008 Krakow, Poland.

Porous Carbons for Hydrogen Storage: Physics, Chemistry and Prospects, J. E. Fischer, Georgetown University, Oct. 9, 2008 (invited).

Monolithic Carbide-derived Carbon Films with Superior Volumetric Capacitance, J. Chmiola, Y. Gogotsi, C. Largeot and P. Simon, *214th Electrochemical Society Meeting,* October 12-16, 2008, Honolulu, HI

Nanostructured Carbons for Energy-Related Applications, Y. Gogotsi, *EPRI Workshop Materials for Next Generation Energy Storage*, October 20-21, 2008, Cleveland, OH

Nanostructured Carbide-Derived Carbons for Energy-Related and Biomedical Applications, Y. Gogotsi, *RUSNANOTECH,* Moscow, Dec. 2-6, 2008

High Specific Surface Area Carbon from Etching of SiCN Ceramics, S.-H. Yeon, P.Reddington, P. Colombo, J. E. Fischer, Y.Gogotsi, *33rd International Cocoa Beach Conference on Advanced Ceramics and Composites*, Daytona Beach, FL, January 2009

Development of Carbide-Derived Carbons for Supercapacitors, Y. Gogotsi, (keynote), *ISEE'Cap09, First International Symposium on Enhanced Electrochemical Capacitors*, 29 June – 2 July 2009, Nantes, France.

Supercapacitors for Electrical Energy Storage and Harvesting, Yury Gogotsi, (invited), *US-Korea Conference (UKC) 2009 on Global Sustainability*, Raleigh, NC, July 16-19, 2009

Molecular Modeling of Disordered Micro-Porous Carbons: Atomistic Models, Adsorption and Diffusion, Jeremy Palmer, Ying-Chun Liu, Joshua D. Moore, John K. Brennan, Yury Gogotsi, John Fischer and Keith E. Gubbins*, 8th Torun Carbon Symposium of the Polish Carbon Society*, 2-5 Sept 2009.

Understanding the Structure of Titanium Carbide Derived Carbons through Experiment and Molecular Simulation, Jeremy C. Palmer, Anna Llobet, John E. Fischer, Yury Gogotsi and Keith E. Gubbins, *LANSCE Users Group Meeting* Sept. 29-30, Los Alamos National Laboratory, New Mexico.

Atomic-Scale Impurity Identification and 3-D Morphology of Mesoporous Carbide-Derived Carbons, Ilke Arslan, Scarlett Widgeon, Mhairi Gass, Andrew Bleloch, Sun-Hwa Yeon, and Yury Gogotsi, *2009 MRS Spring Meeting*, San Francisco, April 2009.

Molecular Modeling and Simulation of Titanium Carbide Derived Carbons, *Jeremy Palmer*, Sun-Hwa Yeon, Anna Llobet, Keith Gubbins, John Fischer and Yuri Gogotsi, *Pacific Basin Conference on Adsorption Science and Technology*, Singapore, May 2009.

Local structure of microporous carbide-derived carbons from radial distribution function analysis: Correlations with hydrogen storage, Anna Llobet, Sun-Hwa

Yeon, Yury Gogotsi, Jason Simmons, Keith Gubbins and <u>John E. Fischer,</u> *Carbon 2009,* Biarritz, June 2009.

Enhanced Methane Storage of Chemically and Physically Activated Carbide-Derived Carbon, *Sun-Hwa Yeon,* Sebastian Osswald, Yury Gogotsi, Jonathan P. Singer, Jason M. Simmons, John E. Fischer, M.A. Lillo-Ródenas, A. Linares-Solano, *Workshop on Porous Materials,* Rutgers University June 2009.

Carbide Derived Carbon as a Chemical and Biological Sorbent, Y. Gogotsi, *Army Research Office Workshop on Dynamics and Chemistry of Surfaces and Interfaces,* Savannah, GA, June 2009.

Special Recognitions & Awards

Nanotech Briefs "Nano 50" award in the Technology category to Drexel University for development of Carbide-Derived Carbons. Nanotech Briefs magazine is the monthly digital publication from the publishers of NASA Tech Briefs. "Nano 50" recognizes the top 50 technologies, products, and innovators that have significantly impacted, or are expected to impact, the state of the art in nanotechnology. (2006).

Eleven patents filed by Y-Carbon, one cited above resulting directly from this award. For completeness the others are listed here to further demonstrate the wide range of applications for CDCs.

1. Process for producing nanoporous carbide derived carbon with large specific surface area, PCT/US2006/045154.
2. Nanocellular high surface area material and methods for use and production thereof, US 2006/0165584 A1, PCT/US2006/014048.
3. Methods for bulk synthesis of single-wall carbon nanotubes, PCT/US2005/021017.
4. Nanoporous carbon with tunable pore size, PCT/US2004/021382.
5. Nanoporous carbonaceous membranes and related methods, PCT/US2007/011442.
6. Methods for increasing volumetric and gravimetric energy of supercapacitors through subnanometer pore size control.
7. Method for selecting the pore size for a given electrolyte and an electrolyte for a given porous carbon material for supercapacitor electrodes.
8. Mesoporous carbon, PCT/US2006/047129.
9. Chlorine-Loaded Carbide Derived Carbon with Bactericidal Properties, US Provisional Patent Application No. 60/708,134.
10. Electrocatalyst for fuel cells, application filed.

Yury Gogotsi elected fellow of the American Ceramic Society (2007).

Taner Yildirim received an <u>Arthur S. Flemming Award</u>, given for excellence in federal service (2007). His citation reads: "For his outstanding accomplishments

in investigations of the properties of materials using neutron scattering experiments and associated first-principles calculations. His work has provided profound insights into the properties of superconductors and hydrogen storage materials, offering promise for future energy technologies"

Taner Yildirim won the 2007 United States Department of Commerce Gold Medal for distinguished performance characterized by extraordinary, notable or prestigious contributions that impact the mission of the Department of Commerce and/or one operating unit and which reflect favorably on the Department.

The editors of Technology Review magazine named Dr. Ranjan Dash one of this year's TR35, a group of the world's top young innovators. He was profiled in Technology Review. (2008)

Y-Carbon (http://www.y-carbon.us/) has received two SBIR Phase 1 grants from NSF and ONR, and a $50,000 grant from Ben Franklin Technology Partners (2008).

Drexel University and Y-Carbon received a 2009 R&D 100 Award for Tunable Nanoporous Carbon.
Taner Yildirim was elected Fellow of the American Physical Society (2008).

Taner Yildirim won the prestigious Special Award for 2009 from Tubitak, the Scientific and Technological Research Council of Turkey.

Drexel University Trustee Chair Professor Yury Gogotsi was invited by the Materials Research Society to guest-edit a special issue of Journal of Materials Research devoted to Energy Storage Materials in 2010.